Article

Passively Sampled Environmental Films Shows Geographic Variability and Host Variety of Microorganisms

Jacob S Grant, Patrick M Richards, Christopher Robert Anderton, Zihua Zhu, Timothy E. Mattes, and Scott K Shaw

ACS Earth Space Chem., **Just Accepted Manuscript** • DOI: 10.1021/acsearthspacechem.9b00234 • Publication Date (Web): 14 Oct 2019

Title:
Passively Sampled Environmental Films Shows Geographic Variability and Host Variety of Microorganisms

Authors:

1) Jacob S. Grant, Department of Chemistry, University of Iowa, Iowa City, IA 52242, jacob-grant@uiowa.edu
2) Patrick M. Richards, Department of Civil and Environmental Engineering, University of Iowa, Iowa City, IA 52242, patrick-richards-1@uiowa.edu
3) Christopher R. Anderton, Environmental Molecular Sciences Laboratory, Pacific Northwest National Laboratory, Richland, WA 99354, Christopher.Anderton@pnnl.gov
4) Zihua Zhu, Environmental Molecular Sciences Laboratory, Pacific Northwest National Laboratory, Richland, WA 99354, Zihua.Zhu@pnnl.gov
5) Timothy E. Mattes, Department of Civil and Environmental Engineering, University of Iowa, Iowa City, IA 52242, tim-mattes@uiowa.edu
6) Scott K. Shaw*, Department of Chemistry, University of Iowa, Iowa City, IA 52242, scott-k-shaw@uiowa.edu

Abstract

Environmental films are ubiquitous coatings that form on virtually all surfaces exposed to the troposphere. This work analyzes large molecular weight species in native environmental films acquired at three collection sites in the vicinity of Iowa City, Iowa, USA that include an urban residence, a wooded area, and a metropolitan building rooftop. The films are developed for up to twelve months on polished silicon wafer substrates housed in flat-plate passive samplers. Film composition was assessed by Fourier transform ion cyclotron resonance secondary ion mass spectrometry (FTICR-SIMS), and spatially resolved chemical morphology was analyzed via time-of-flight secondary ion mass spectrometry (ToF-SIMS) imaging. Mass analysis spanning up to *m/*z 2,000 included detection of a variety of organic and inorganic compounds. We characterize MS data with PCA to identify variability between the collection sites and the respective films generated therein, where we detected a variety of organic and biotically generated species consistent with fungal and bacterial microorganisms. Film collection site as well as deposition time contribute to spectral variability, suggesting that geographic location as well as seasonal diversity may affect composition. SIMS analyses were complemented with microscopy and SYBR-Safe staining to highlight biological microorganisms within the films, which include evidence of fungi, protozoa, and bacteria. SIMS imaging also reveals domains concentrated with fragments indicative of proteinaceous macromolecules and microbial biomass, characteristic of biological presence within the film.

Key Words

Environmental Film, Mass spectrometry, Speciation, Imaging, Morphology, Fate and transport

Introduction

"Environmental film" or "urban film" is a term given to exterior surface films in the environment resulting from deposition of suspended atmospheric particulate matter (PM) and individual molecules onto man-made structures and vegetation. The films' chemical compositions are based on the complex profile of PM, volatile organic compounds (VOCs) reacting to form lower volatility secondary organic aerosols (SOAs), semivolatile organic compounds (SVOCs), and biogenic volatile organic compounds (BVOCs) that similarly react to form SOA. Each of these classes of material can exist for extended times suspended in the atmosphere before depositing across the Earth's surfaces. Different geographic locations are expected to be represented by the variety of chemical species present within the films, especially considering factors such as proximity to nearby point-emission sources.[1-7] Further, the capture efficiency of the surface is expected to be significantly affected by the film composition, which can effectively increase or decrease further deposition/adsorption of new material, effecting a film's accumulation and chemical profile. This is important as it affects SVOC partitioning into an organic phase that might not otherwise be present on a solid surface. This added capacity due to the environmental film is incredibly important because it enhances surfaces' roles in the fate and transport of persistent organic pollutants (POPs)[2, 8], as well as their roles in generating atmospherically-relevant reactions based on studies of model films[9-13] and native films.[14-16]

In addition to significant chemical complexity and variability, film composition is continuously altered by environmental factors such as UV-initiated oxidation, exposure to tropospheric radicals, or climatological factors such as wind, precipitation, and swings in temperature and humidity. These factors alter the films' compositions and behaviors, affecting changes in SVOC partitioning, total film mass accumulation or loss, and capture efficiency of airborne aerosol materials.[17-19] Ultimately, a wide range of dynamic physical and chemical factors dictate the impact of environmental films on mass transport, including possibly unique POPs degradation pathways.[20]

Environmental films' chemical profiles are characterized in several prior reports. Depending on the location where the film was formed, the composition ranges from 5% to 50% organic components by mass, and can be divided into three approximately equal fractions of aliphatics, carbohydrates, and aromatics and carbonyls. The balance of the film mass is reported to be inorganic materials including primarily silicate minerals, nitrates, sulfates, and metals.[4, 7, 21, 22] The ambiguity in organic composition presents a large degree of uncertainty in reactivity studies and chemical transport models. For example, POPs are an important class of compounds that can accumulate in environmental films due to their resistance to environmental degradation. Several POPs, including polychlorinated biphenyls (PCBs),[23-26] polycyclic aromatic hydrocarbons (PAHs),[27, 28] and polybrominated diphenyl ethers (PBDEs)[1, 29, 30] have been detected in native environmental films. The multimedia urban model, an example representative system, has also been extensively utilized to characterize the effect the films have on the transport of POPs.[20, 31-38] Given the ubiquitous presence of environmental films, the immense surface area they cover globally, and their propensity to uptake POPs, it is clear that they represent a significant impact on environmental and human health, yet their composition and dynamics remain largely uncharacterized.

While earlier reports[4, 7, 21, 22] provide valuable data regarding the elemental or functional group composition of environmental films *en masse*, they do not provide specific, large molecular weight chemical analyses of anthropogenic and biogenic contributions to film composition. Anthropogenic emissions that might accumulate in environmental films vary widely, but largely include hydrocarbon products of incomplete fuel combustion,[39] as well as restaurant cooking emissions,[40] whereas biogenic emissions include reduced carbon species from plant emission[41] and proteinaceous biomass from bacteria and fungi.[42]

Here, we characterize the chemical composition of native environmental films collected passively from three different sampling sites for times ranging from 1-12 months. We focused on the large molecular weight composition of the films and examine variability between the collection sites and time points. Composition was characterized using Fourier transform ion cyclotron resonance secondary ion mass spectrometry (FTICR-SIMS) and chemical surface morphology data obtained using time-of-flight secondary ion mass spectrometry (ToF-SIMS) imaging, which builds upon a preliminary report by our group examining primarily low mw species.[43] The results show ion fragments with mass-to-charge (*m/z*) ratios indicative of a large variety of organic compounds, including hydrocarbons as well as nitrogen and phosphorus containing species. The variability in the FTICR-SIMS data is described via principal component analysis (PCA), which indicates that film deposition time and potentially seasonal variations impact film composition. Seasonal changes are expected to affect levels of PM, VOCs, SVOCs, and BVOCs present in the atmosphere,[44-47] and we are interested in understanding how these atmospheric compositions affect chemistry within the film. Finally, to assess the biological contributors to environmental films we utilized DNA staining via SYBR-Safe and fluorescence microscopy.

Experimental

Substrate Preparation: Polished silicon wafers (Silicon Valley Microelectronics, Santa Clara, CA, USA) cut into ca. 6.5 cm^2 pieces are used as substrates for the dry and wet deposition of PM to form native environmental films. Silicon wafers are chosen as suitable substrates because they contain an oxide layer similar to that of window glass, and they are amenable to the analytical methods discussed herein. We note that the porous nature of many outdoor surfaces, which allows for enhanced sorption surface area and intercalation of atmospheric species able to fit into the pores, is not captured by the wafers, but submit that the wafers are suitable proxies for environmental surfaces. The wafers are 525 ± 25 μm thick with a 100 ± 5 nm thermally grown oxide layer on the surface. The substrates are cleaned via Jelight (Irvine, CA, USA) Model 42 UVO cleaner for 10 min, after which they are sonicated in ultrapure isopropyl alcohol (IPA) for 5 min, dried under a stream of ultrapure nitrogen gas, and stored in IPA-cleaned, covered quadrant petri dishes. The substrates are placed in flat-plate, passive samplers (described previously and summarized below)[48] for native film collection, after which they are transported and stored in sealed petri dishes until analysis. Glassware utilized for native film analysis is cleaned via extended soaking in Nochromix followed by 50% nitric acid (both >12 hrs), rinsing with ultrapure water (18.2 MΩ cm, <5 ppb TOC content) between each bath and boiling ultrapure water after the nitric acid bath. The glassware used is cleaned prior to each use to ensure minimal contamination onto the substrates and therefore the native film samples.

Flat-Plate Passive Sampling of Native Environmental Films: A passive sampling apparatus is used to closely emulate the deposition of tropospheric PM without outside perturbation. The sampling apparatus consists of a large upper and smaller lower plate of aluminum.[48] Briefly, eight substrates for film collection are placed on the lower plate, in the ~2 cm gap between plates, to shield them from rainfall (although they are still exposed to humid air), and the apparatus is mounted ca. two meters from ground level. The collection sites are chosen based on geographic proximity to biogenic and anthropogenic emission sources, which allows for the analysis of differing chemical profiles unique to each site. The first collection site outside near a residential neighborhood (labeled "urban residence"; latitude, longitude, elevation: 41.648443°, -91.576112°, 2 m, respectively), chosen to profile an area of limited human activity. The second collection site is a wooded area near the urban residence ("wooded area"; 41.686360°, -91.586003°, 2 m), which was chosen to profile an area with increased plant life, and different biogenic contributors. The third collection site is located on the roof of a metropolitan building in downtown Iowa City ("metropolitan"; 41.663634°, -91.537635°, rooftop) to profile an area of increased anthropogenic emissions and human activity. Films were collected after 1-52 weeks as specified in figures, with samples collected at: 1 week, 2 weeks, 1 month, 3 months, 6 months, 12 months. This study was conducted between January 2016 and January 2017. Temperature and humidity data for this collection period is presented in an earlier report[43] on these native film samples.

Fourier Transform Ion Cyclotron Resonance Secondary Ion Mass Spectrometry (FTICR-SIMS): FTICR-SIMS measurements are performed at the Environmental Molecular Sciences Laboratory (EMSL) at Pacific Northwest National Laboratory (PNNL). A C_{60} primary ion (Ionoptika, Chandlers Ford, Hampshire, UK) coupled to a 7 Tesla solariX FTICR mass spectrometer (Bruker Daltonics, Billerica, MA, USA) via a custom built housing, as detailed elsewhere,[49, 50] is utilized for measuring the chemical composition of these films. The instrument is externally calibrated on an Indium film standard, where the error is $\leq$3 ppm on each of the In^+ clusters detected and used for calibration. All analyses are performed with C_{60}^+ primary ions at 40 keV, with an ion beam current of ~810 pA, and a beam size of 21 μm, where secondary ions are accumulated for 1 s prior to FTICR-MS analysis. The C_{60} ionization source, the parameters of which are chosen for standard detection of proteinaceous macromolecules,[49, 51] is utilized to provide a softer ionization and result in much larger fragments (up to 1,800 m/z) due to the different type of primary ion beam utilized, which provides more information regarding the origin of the fragments (lipids, hydrocarbons, etc.). The scan area is on the order of 1 mm^2, and n$\geq$4 spots are obtained for each substrate. The imaging area is randomly chosen for each substrate, and each area was characterized in random order by the instrument.[49] Positive-ion mode mass spectral data is collected from *m/z* 150-2000 with a mass resolving power of ~63,000 at *m/z* 400. Spectra are analyzed using Bruker Data Analysis software. Potential molecular formulae for the FTICR-SIMS data are assigned using the Molecular Formula Calculator v1.2.3,[50, 52] with a mass accuracy upper limit of 5.0 ppm, and the charge is set to 1+ (2+ and 3+ are used if 1+ yields no molecular formulae). The elemental constraints are set to provide formulae realistic to natural organic matter,[53] including sodium adducts common in positive ion mode mass spectrometry. Radicals are allowed in determining potential formulae. Formula error and double bond equivalence (DBE) are also reported.

Time-of-Flight Secondary Ion Mass Spectrometry (ToF-SIMS) Imaging: ToF-SIMS measurements are also performed at EMSL-PNNL with a TOF.SIMS5 instrument (IONTOF GmbH, Münster, Germany). The analysis beam is a 25 keV Bi_3^+ beam (0.57 pA current, 10 kHz pulse frequency)

focused to a diameter of ~5 μm, which is scanned over a 500 x 500 μm^2 area at a resolution of 256 lines/mm (128 x 128 pixels). The data collection time is ~160 sec per spectrum and spectra are obtained in positive-ion mode. The total ion dose is kept under the static limit, where only surface molecules (<2 nm deep) are collected. During data collection, a low energy electron flood gun (10 eV, ~1.0 μA current) compensates for surface charging. The analysis chamber pressure is maintained at ~ 2×10^{-8} mbar. Spectra and images are analyzed using SurfaceLab 6 software. Representative features are presented for n≥6 in positive ion mode for each substrate. Additional ToF-SIMS experimental details have been previously detailed.[43, 54]

Principal Component Analysis (PCA): PCA was performed utilizing the statistical analysis package of MetaboAnalyst 4.0.[55-67] The mass tolerance was set to 0.005 *m/z* to account for slight instrument deviation in assigning an individual peak, and ensures this deviation is not falsely assessed as variability in the data. The data filtering was set to none, and data normalization was set to normalize by the total spectrum intensity and mean center the data, in accordance with previous reports of PCA on SIMS data.[68] Scores plots (n≥4 for each sample type) describe the variance between data sets.

DNA Staining and Microscopy: Native environmental films are stained and imaged directly on the silicon wafers. SYBR-Safe dye (Invitrogen, Carlsbad, CA) is diluted in tris-acetate EDTA buffer (40x final concentration).[69] The wafers are flooded with dye solution, pressed with a coverslip, and incubated for 15 min in the dark.[69] Unbound dye is rinsed from the film with ultrapure water. The films are imaged at the University of Iowa Central Microscopy Research Facility (CMRF) using an Olympus (Shinjuku, Tokyo, Japan) BX61 epifluorescence microscope equipped with a green fluorescent protein (GFP) fluorescence filter. Magnification extends up to 100x and is noted on each individual image. Unstained samples are also examined for autofluorescence. Representative features are presented for n≥20 images per substrate.

Results and Discussion

Representative FTICR-SIMS data consisting of the prevalent peaks observed at each sample collection site over six months of deposition are shown in **Figure 1**. The spectra exhibit several common peaks, as well as subtle differences more easily visualized in the overlay spectrum presented in **Figure S1**. Spectral subtraction is utilized to exclude the peaks common to all the samples, and the peaks unique to each collection site are reported in **Figure 2**. As the sampled film area is on the order of 1 mm^2, the spectra are more representative of the bulk film composition, rather than of individual microdomains that exist within these very heterogenous films. The use of the C_{60}^+ primary ions results in a multitude of secondary ion fragments from the native film samples spanning up to *m/z* 2000. Potential molecular formula for the common and unique fragments exhibiting the largest intensity are presented in **Table 1**. The fragments' molecular formula are consistent with similar FTICR-SIMS analysis on tissues, cells, and microorganisms that are likely to constitute natural organic matter (NOM) in the environment and contribute to environmental film formation.[70, 71] Furthermore, the potential molecular formulae proposed here generally match in composition (relative amounts of carbon, hydrogen, nitrogen, oxygen, and phosphorous) to lipid species identified in the aforementioned reports.[70, 71] The double bond equivalence (DBE) is also reported to ensure realistic molecular formulae determination, and the DBE match well with previous reports for NOM analysis.[72] The large amount of molecular

formulae identifying organic matter is also in agreement with reported local data of atmospheric material, in which the largest contributor (estimated 39 ± 11%) of fine particulate matter mass is attributed to organic matter.[73] While the silicon wafer substrates used in this analysis have been reported to accumulate organic impurities,[74-77] these are primarily much smaller and more volatile organics than what we observe here. The fragments common to our three collection sites are larger than 600 Daltons in mass. The FTICR-SIMS data is collected under high vacuum conditions, so contributions from volatile organics in this data is expected to be minimal. While assigning exact structures from m/z data reported here is challenging, realistic formulae are provided with excellent instrumental resolution.

We use principal component analysis (PCA) to evaluate variability of the FTICR-SIMS data. PCA[78-80] is a multivariate analysis method that describes the variability within a set of samples by aligning the data on a new set of principal component axes (PCs) based on the maximum directions of variance. For FTICR-SIMS data, the samples are individual spectra and the variables are the intensities of mass channels corresponding to a specific *m/z*.[68] Scores plots show the relationship between samples, and the loadings show how the variables describe the separation. The first PC (PC1) is defined as that PC which describes the most variability in the data set; PC2 then defines the second most variability, and so on. Scores plots showing PCs 1 and 4 are presented in **Figure 3** for FTICR-SIMS data collected on substrates at each collection site at a constant time point of six months (additional PCA plots are shown in SI). Here, we observe that PC1 captures the majority of the variance at 86.6%, and PCs 2-5 capture 6.0%, 3.1%, 1.7%, and 1.1%, respectively. The loadings in **Figure 4** indicate that m/z 816.5925 and 778.6451 are more related to the wooded area site while m/z 648.7175 and 997.5444 are more related to the metropolitan and urban residence sites. The variability is due to both the presence or absence of ion peaks at each site, typically described by the higher PCs, as well as intensity differences between peaks present at each of the three sites, described by the lower PCs. Beginning with PC5, the loadings indicate that variance is explained by changing ion fragment intensity for fragments that are observed at all sampling locations. The trend of higher PCs describing variability in ion fragments while lower PCs describe variability in fragment intensity or surface coverage has been previously reported for SIMS data.[81-85] Ultimately, the scores plot supports the conclusion that the wooded area site exhibits chemical variability when comparted to the other samples. This is reasonable and expected due to the presence of many unique fragments in the mass spectral data as shown in **Figure 2**.

Figure 5 presents a scores plot of the first two PCs describing the variability between collection sites including separate data for variable exposure times (one-, three-, and six-months). The variances described by PCs 1-5 are 47.1%, 28.4%, 7.0%, 6.2%, and 2.3%, respectively. The grouping of the scores plot indicates that the one- and six-month samples from the wooded area site as well as the six-month sample from the urban residence site exhibit significant variability relative to the rest of the samples. This may indicate variability in film composition of the six-month samples (exposed January to June) due to seasonal variation, as the one- and three-month samples are collected during the winter months while the six-month film collections extends into the spring and summer months. Seasonal variations are known to affect levels of PM and VOCs present in the atmosphere,[44-47] including particulate carbon as well as common SO_x, NO_x, and NH_4^+ ions. The presence of environmental microorganisms are also known to be influenced by seasonal variations as well as geographical location.[86-88] While additional studies are underway to probe these effects further, we can predict that similar changes are likely in the surface film

compositions. The rest of the sample classes exhibit relatively low variability based on the score groupings, though clustering of like samples within these sample sets is observed. The loading plots indicate that the variance described by PCs 1-3 is due to ion fragments present in only a few of the sample sets. The large variance described by PC2 is indicative of ion fragments present in approximately half of the samples. The variance described by PC4 is due to intensity differences among fragments present in the majority of the samples. **Figure 6** presents a loading plot for PCs 1 and 2, and characterizes the variability in the data described by these PCs. This trend matches what was previously observed here and in similar analyses,[81-85] namely that the largest variability in FTICR-SIMS data is attributed to presence (or absence) of specific fragments at specific sites, while smaller variability is due to differences in intensity of fragments that are common to all the samples analyzed. The scores plot, therefore, indicates that the one- and six-month samples from the wooded area site as well as the six-month sample from the urban residential site exhibit higher variability relative to the other samples, and this variability is due to the presence of unique molecular ion fragments.

This analysis is an important first step in characterizing the large molecular weight composition of native environmental films. Additional collection sites, samples, and fine control of seasonal variability will provide better details on chemical profile of native environmental films. Expansion of the multivariate analyses with PCA across these variables has the potential to provide stronger correlations and deeper understanding of this complex system, possibly contributing high-quality data in the form of a library or database for environmental films, to which newly obtained samples can be added and compared. To this end **Figure S2-S4** present the raw FTICR-SIMS data for each collection site at each time point. These spectra show qualitative similarities of prominent peaks and relative signal intensity of secondary ion fragments at each time point.

To further characterize the profile of proteinaceous macromolecules and biomass on the native environmental film samples, representative ToF-SIMS images shown in **Figure 7** show three- and six-month urban residential collection samples. The SIMS ion images a common secondary ion fragment species annotated as $C_3H_8N^+$. The species is a marker of biologically-fixed nitrogen often incorporated in proteins and a number of different lipid classes.[89] The ion intensity shown is scaled to be equivalent for each image, and we observe sharply defined domains of the carbon-hydrogen-nitrogen fragment that increase in surface coverage and intensity as the native films deposit for longer times. This represents an accumulation of biological material which we hypothesize to be from bacterial or fungal colonies growing on the substrate to produce these sharply defined domains. We would expect purely atmospheric deposition of species to result in evenly distributed microorganisms of smaller cluster sizes spread across the surface. Growth of these biological species suggests a significant, biogenic contribution to film composition that has not been studied in previous environmental film reports.

We also include staining and fluorescence microscopy images of the films and compare the observed features to autofluorescent species on an unstained environmental film. SYBR-Safe is a cyanine dye with a very high binding affinity for nucleic acids, relatively low affinity for other biopolymers, and low intrinsic fluorescence when not bound to nucleic acids,[90] making it useful for imaging microorganisms. The images shown in **Figure 8** are representative of many images we acquired for microorganisms in the environmental films. These include large rectangular cells forming branched filaments, characteristic of fungi,[67, 91] as well as pairs or clusters of large (>5μm)

features with variable morphology, likely representing various species of protozoa cells.[92] The relatively large size of these cells, in addition to brightly stained nuclei indicate that they are eukaryotic. In addition, there are numerous bacterial cells, which can be identified by their smaller sizes (<3μm).[92] We note that the bacterial cells are often arranged in pairs or chains and closely associated with the fungal filaments.

Conclusions

In this manuscript, we have presented a characterization of native environmental films developed passively at three different urban and rural collection sites, evaluating a mass spectral data over a large m/z range. We emphasize the extremely complex and diverse composition of these films, including a variety of organic and biological species revealed by FTICR-SIMS data, and highlight the subtle differences in composition between each collection site. The FTICR-SIMS data is supplemented with potential molecular formulae for the most intense fragments as well as PCA to describe the variability between collection sites. ToF-SIMS images are utilized to show spatially resolved chemical information of mass fragments indicative of biological presence, and highlight the complex chemical profile and domains present in native environmental films. The biological presence on the environmental films is further characterized via DNA staining and fluorescence microscopy. This work provides essential data in characterizing the time and location-dependent analysis of environmental films. Further research will expand the composition analysis with high resolution mass spectrometry imaging to characterize films at more populated and remote collection sites. A detailed chemical profile of environmental films is critical to completely assess their reactivity with other environmental agents, including POPs.

Supporting Information

Figure S1, FTICR-SIMS data overlay
Figures S2, S3, and S4, Raw FTICR-SIMS data of the wooded, metropolitan roof, and urban residential sites respectively
Figures S5-S8: Scores plots and corresponding loading plots for collection site PC1 vs PC2, PC3, PC4, and PC5
Figures S9-S12: Scores plots and corresponding loading plots for collection site and deposition time PC1 vs PC2, PC3, PC4, and PC5

Acknowledgements

The authors would like to acknowledge Prof. Tom Peters and Prof. Betsy Stone for providing flat plate passive samplers and excellent advice regarding the sampling of particulate matter, and Dr. Brian Dess for advice and assistance in conducting PCA on the SIMS data. Funding was provided by the UIowa Graduate College, the UIowa Center for Global & Regional Environmental Research (CGRER), the UIowa Center for Health Effects of Environmental Contamination (CHEEC), the Department of Defense Army Research Office Proposal No. 71600-CH, and the Nuclear Regulatory Commission (NRC) graduate fellowship program (NRC-HQ-84-14-G-0037). A portion of this work was performed at EMSL, a national scientific user facility sponsored by the Office of Biological and Environmental Research (BER), U.S. Department of Energy (DOE).

EMSL is located at PNNL, a multidisciplinary national laboratory operated by Battelle for the U.S. DOE.

References

1. Butt, C. M.; Diamond, M. L.; Truong, J.; Ikonomou, M. G.; Helm, P. A.; Stern, G. A., Semivolatile organic compounds in window films from lower Manhattan after the September 11th World Trade Center attacks. *Environmental Science and Technology* **2004,** *38*, 3514-3524.
2. Diamond, M. L.; Gingrich, S. E.; Fertuck, K.; McCarry, B. E.; Stern, G. A.; Billeck, B.; Grift, B., Evidence for organic film on an impervious urban surface: Characterization and potential teratogenic effects. *Environmental Science and Technology* **2000,** *34*, 2900-2908.
3. Gingrich, S. E.; Diamond, M. L.; Stern, G. A.; McCarry, B. E., Atmospherically derived organic surface films along an urban-rural gradient. *Environmental Science and Technology* **2001,** *35*, 4031-4037.
4. Lam, B.; Diamond, M. L.; Simpson, A. J.; Makar, P. A.; Truong, J.; Hernandez-Martinez, N. A., Chemical compostion of surface films on glass windows and implications for atmospheric chemistry. *Atmospheric Environment* **2005,** *39*, 6578-6586.
5. Law, N. L.; Diamond, M. L., The role of organic films and the effect on hydrophobic organic compounds in urban areas: An hypothesis. *Chemosphere* **1998,** *36*, 2607-2620.
6. Melymuk, L.; Robson, M.; Diamond, M. L.; Bradley, L. E.; Backus, S., Wet deposition loadings of organic contaminants to Lake Ontario: Assessing the influence of precipitation from urban and rural sites. *Atmospheric Environment* **2011,** *45*, 5042-5049.
7. Simpson, A. J.; Lam, B.; Diamond, M. L.; Donaldson, D. J.; Lefebvre, B. A.; Moser, A. Q.; Williams, A. J.; Larin, N. I.; Kvasha, M. P., Assessing the organic composition of urban surface films using nuclear magnetic resonance spectroscopy. *Chemosphere* **2006,** *63*, 142-152.
8. Liu, Q.-T.; Diamond, M. L.; Gingrich, S. E.; Ondov, J. M.; Maciejczyk, P.; Stern, G. A., Accumulation of metals, trace elements and semi-volatile organic compounds on exterior window surfaces in Baltimore. *Environmental Pollution* **2003,** *2003*, 1.
9. Bertram, A. K.; Ivanov, A. V.; Hunter, M.; Molina, L. T.; Molina, M. J., The reaction probability of OH on organic surfaces of tropospheric interest. *Journal of Physical Chemistry A* **2001,** *105*, 9415-9421.
10. Kahan, T. F.; Kwamena, N. O. A.; Donaldson, D. J., Heterogeneous ozonation kinetics of polycyclic aromatic hydrocarbons on organic films. *Atmospheric Environment* **2006,** *40*, 3448-3459.
11. Knopf, D. A.; Mak, J.; Gross, S.; Bertram, A. K., Does atmospheric processing of saturated hydrocarbon surfaces by NO_3 lead to volatilization. *Geophysical Research Letters* **2006,** *33*, L17816.
12. Mak, J.; Gross, S.; Bertram, A. K., Uptake of NO_3 on soot and pyrene surfaces. *Geophysical Research Letters* **2007,** *34*, L10804.
13. Vlasenko, A.; George, I. J.; Abbatt, J. P. D., Formation of volatile organic compounds in the heterogeneous oxidation of condensed-phase organic films by gas-phase OH. *Journal of Physical Chemistry A* **2008,** *112*, 1552-1560.
14. Baergen, A. M.; Styler, S. A.; van Pinxteren, D.; Muller, K.; Herrmann, H.; Donaldson, D. J., Chemistry of urban grime: Inorganic ion composition of grime vs particles in Leipzig, Germany. *Environmental Science and Technology* **2015,** *49*, 12688-12696.
15. Styler, S. A.; Baergen, A. M.; Donaldson, D. J.; Herrmann, H., Organic composition, chemistry, and photochemistry of urban film in Leipzig, Germany. *ACS Earth and Space Chemistry* **2018,** *2*, 935-945.
16. Baergen, A. M.; Donaldson, D. J., Seasonality of the Water-Soluble Inorganic Ion Composition and Water Uptake Behavior of Urban Grime. *Environmental Science & Technology* **2019,** *53*, 5671-5677.
17. Asad, A.; Mmereki, B. T.; Donaldson, D. J., Enhanced uptake of water by oxidatively processed oleic acid. *Atmospheric Chemistry and Physics* **2004,** *4*, 2083-2089.

18. Baergen, A. M.; Donaldson, D. J., Photochemical renoxification of nitric acid on real urban grime. *Environmental Science and Technology* **2013,** *47*, 815-820.
19. Baergen, A. M.; Donaldson, D. J., Formation of reactive nitrogen oxides from urban grime photochemistry. *Atmospheric Chemistry and Physics* **2016,** *16*, 6355-6363.
20. Csiszar, S. A.; Diamond, M. L.; Thibodeaux, L. J., Modeling urban films using a dynamic multimedia fugacity model. *Chemosphere* **2012,** *87*, 1024-1031.
21. Donaldson, D. J.; Kahan, T. F.; Kwamena, N. O. A.; Handley, S. R.; Barbier, C., Atmospheric chemistry of urban surface films. In *Atmospheric Aerosols*, Valsaraj, K. T.; Kommalapati, R. R., Eds. Oxford University Press2009; pp 79-89.
22. McBride, M. B., *Soil Solids: Composition and Structure*. Oxford University Press: New York, 1994.
23. Diamond, M. L.; Hodge, E., Urban contaminant dynamics: From source to effect. *Environmental Science and Technology* **2007,** *41*, 3796-3805.
24. Cotham, W. E.; Bidleman, T. F., Polycyclic aromatic hydrocarbons and polychlorinated biphenyls in air at an urban and rural site near Lake Michigan. *Environmental Science and Technology* **1995,** *29*, 2782-2789.
25. Helm, P. A.; Bidleman, T. F., Current combustion-related sources contribute to polychlorinated naphthalene and dioxin-like polychlorinated biphenyl level and profiles in air in Toronto, Canada. *Environmental Science and Technology* **2003,** *37*, 1075-1082.
26. Wu, R. W.; Harner, T.; Diamond, M. L., Evolution rates and PCB content of surface films that develop on impervious urban surfaces. *Atmospheric Environment* **2008,** *42*, 6131-6143.
27. Unger, M.; Gustafsson, O., PAHs in Stockholm window films: Evaluation of the utility of window film content as indicator of PAHs in urban air. *Atmospheric Environment* **2008,** *42*, 5550-5557.
28. Yu, Y.; Yang, Y.; Wang, Q.; Liu, M., Distribution, sources, and risk assessment of PAHs in organic films on glass window surfaces along the urban-rural gradient in Shanghai, China. *Polycyclic Aromatic Compounds* **2018**, DOI: 10.1080/10406638.2018.1441880.
29. Butt, C. M.; Diamond, M. L.; Truong, J.; Ikonomou, M. G.; ter Schure, A. F., Spatial distribution of polybrominated diphenyl ethers in sourthern Ontario as measured in indoor and outdoor window organic films. *Environmental Science and Technology* **2004,** *38*, 724-731.
30. Cetin, B.; Odabasi, M., Polybrominated diphenyl eithers (PBDEs) in indoor and outdoor window organic films in Izmir, Turkey. *Journal of Hazardous Materials* **2011,** *185*, 784-791.
31. Bogdal, C.; Müller, C. E.; Buser, A. M.; Wang, Z.; Scheringer, M.; Gerecke, A. C.; Schmid, P.; Zennegg, M.; MacLeod, M.; Hungerbühler, K., Emissions of polychlorinated biphenys, polychlorinated dibenzo-p-dioxins, and polychlorinated dibenzofurans during 2010 and 2011 in Zurich, Switzerland. *Environmental Science and Technology* **2014,** *48*, 482-490.
32. Bogdal, C.; Wang, Z.; Buser, A. M.; Scheringer, M.; Gerecke, A. C.; Schmid, P.; Müller, C. E.; MacLeod, M.; Hungerbühler, K., Emissions of polybrominated diphenyl ethers (PBDEs) in Zurich, Switzerland, determined by a combination of measurements and modeling. *Chemosphere* **2014,** *116*, 15-23.
33. Csiszar, S. A.; Diamond, M. L.; Daggupaty, S. M., The magnitude and spatial range of current-use urban PCB and PBDE emissions estimated using a coupled multimedia and air transport model. *Environmental Science and Technology* **2014,** *48*, 1075-1083.
34. Diamond, M. L.; Melymuk, L.; Csiszar, S. A.; Robson, M., Estimation of PCB stocks, emissions, and urban fate: Will our policies reduce concentrations and exposure? *Environmental Science and Technology* **2010,** *44*, 2777-2783.
35. Diamond, M. L.; Priemer, D. A.; Law, N. L., Developing a multimedia model of chemical dynamics in an urban area. *Chemosphere* **2001,** *44*, 1655-1667.
36. Jones-Otazo, H. A.; Clarke, J. P.; Diamond, M. L.; Archbold, J. A.; Ferguson, G.; Harner, T.; Richardson, G. M.; Ryan, J. J.; Wilford, B., Is house dust the missing exposure pathway for PBDEs? An

analysis of the urban fate and human exposure to PBDEs. *Environmental Science and Technology* **2005,** *39*, 5121-5130.

37. Priemer, D. A.; Diamond, M. L., Application of the multimedia urban model to compare the fate of SOCs in an urban and forested watershed. *Environmental Science and Technology* **2002,** *36*, 1004-1013.

38. Rodgers, T. F. M.; Truong, J. W.; Jantunen, L. M.; Helm, P. A.; Diamond, M. L., Organophosphate ester transport, fate, and emissions in Toronto, Canada, estimated using an updated multimedia urban model. *Environmental Science and Technology* **2018,** *52*, 12465-12474.

39. Mendez, S.; Kashdan, J.; Bruneaux, G.; Thirouard, B., Formation of unburned hydrocarbons in low temperature diesel combustion. *SAE International Journal of Engines* **2010,** *2*, 205-225.

40. Zhao, Y.; Hu, M.; Slanina, S.; Zhang, Y., The molecular distribution of fine particulate organic matter emitted from Western-style fast food cooking. *Atmospheric Environment* **2007,** *41*, 8163-8171.

41. Guenther, A. B.; Jiang, X.; Heald, C. L.; Sakulyanontvittaya, T.; Duhl, T.; Emmons, L. K.; Wang, X., The model of emissions of gases and aerosols from Nature version 2.1 (MEGAN2.1): An extended and updated framework for modeling biogenic emissions. *Geoscientific Model Development* **2012,** *5*, 1471-1492.

42. Oldham, W. J.; Hanson, S. K.; Lavelle, K. B.; Miller, J. L., Distribution of neptunium and plutonium in New Mexico lichen samples (*Usnea arizonica*) contaminated by atmospheric fallout. *Journal of Radioanalytical and Nuclear Chemistry* **2016,** *307*, 2079-2084.

43. Grant, J. S.; Zhu, Z.; Anderton, C. R.; Shaw, S. K., Physical and Chemical Morphology of Passively Sampled Environmental Films. *ACS Earth and Space Chemistry* **2019,** *3*, 305-313.

44. Guenther, A., Seasonal and spatial variations in natural volatile organic compound emissions. *Ecological Applications* **1997,** *7*, 34-45.

45. Ho, K. F.; Lee, S. C.; Cao, J. J.; Chow, J. C.; Watson, J. G.; Chan, C. K., Seasonal variations and mass closure analysis of particulate matter in Hong Kong. *Science of the Total Environment* **2006,** *355*, 276-287.

46. Schauer, C.; Niessner, R.; Pöschl, U., Polycyclic aromatic hydrocarbons in urban air particulate matter: Decadal and seasonal trends, chemical degradation, and sampling artifacts. *Environmental Science and Technology* **2003,** *37*, 2861-2868.

47. Shen, Z.; Arimoto, R.; Cao, J.; Zhang, R.; Li, X.; Du, N.; Okuda, T.; Nakao, S.; Tanaka, S., Seasonal variations and evidence for the effectiveness of pollution controls on water-soluble inorganic species in total suspended particulates and fine particulate matter from Xi'an, China. *Journal of the Air & Waste Management Association* **2008,** *58*, 1560-1570.

48. Ott, D. K.; Peters, T. M., A shelter to protect a passive sampler for coarse particulate matter, $PM_{10-2.5}$. *Aerosol Science and Technology* **2008,** *42*, 299-309.

49. Smith, D. F.; Kiss, A.; Leach III, F. E.; Robinson, E. W.; Paša-Tolić, L.; Heeren, R. M. A., High mass accuracy and high mass resolving power FT-ICR secondary ion mass spectrometry for biological tissue imaging. *Analytical and Bioanalytical Chemistry* **2013,** *405*, 6069-6076.

50. Smith, D. F.; Robinson, E. W.; Tolmachev, A. V.; Heeren, R. M. A.; Paša-Tolić, L., C_{60} secondary ion Fourier transform ion cyclotron resonance mass spectrometry. *Analytical Chemistry* **2011,** *83*, 9552-9556.

51. Winograd, N., The magic of cluster SIMS. *Analytical Chemistry* **2005,** *77*, 142A-149A.

52. Coppo, R. L.; Zanoni, K. P. S.; Iha, N. Y. M., Unraveling the luminescence of new heteroleptic Ir(III) cyclometalated series. *Polyhedron* **2019,** *163*, 161-170.

53. Koch, B. P.; Dittmar, T., From mass to structure: An aromaticity index for high-resolution mass data of natural organic matter. *Rapid Communications in Mass Spectrometry* **2006,** *20*, 926-932.

54. Fu, Y.; Zhang, Y.; Zhang, F.; Chen, J.; Zhu, Z.; Yu, X.-Y., Does interfacial photochemistry play a role in the photolysis of pyruvic acid in water? *Atmospheric Environment* **2018,** *191*, 36-45.

55. Chong, J.; Xia, J., MetaboAnalystR: An R package for flexible and reproducible analysis of metabolomics data. *Bioinformatics* **2018,** *27*, 4313-4314.

56. Chong, J.; Soufan, O.; Li, C.; Caraus, I.; Li, S.; Bourque, G.; Wishart, D. S.; Xia, J., MetaboAnalyst 4.0: Towards more transparent and integrative metabolomics analysis. *Nucleic Acids Research* **2018,** *46*, W486-494.
57. Xia, J.; Wishart, D. S., Using MetaboAnalyst 3.0 for comprehensive metabolomics data analysis. *Current Protocols in Bioinformatics* **2016,** *55*, 14.10.1-14.10.91.
58. Xia, J.; Sinelnikov, I.; Han, B.; Wishart, D. S., MetaboAnalyst 3.0 - making metabolomics more meaningful. *Nucleic Acids Research* **2015,** *43*, W251-257.
59. Xia, J.; Mandal, R.; Sinelnikov, I.; Broadhurst, D.; Wishart, D. S., MetaboAnalyst 2.0 - a comprehensive server for metabolomic data analysis. *Nucleic Acids Research* **2012,** *40*, W127-133.
60. Xia, J.; Wishart, D. S., Web-based inference of biological patterns, functions and pathways from metabolomic data using MetaboAnalyst. *Nature Protocols* **2011,** *6*, 743-760.
61. Xia, J.; Wishart, D. S., Metabolomic data processing, analysis, and interpretation using MetaboAnalyst. *Current Protocols in Bioinformatics* **2011,** *34*, 14.10.1-14.10.48.
62. Xia, J.; Psychogios, N.; Young, N.; Wishart, D. S., MetaboAnalyst: A web server for metabolomic data analysis and interpretation. *Nucleic Acids Research* **2009,** *37*, W652-660.
63. Xia, J.; Broadhurst, D.; Wilson, M.; Wishart, D. S., Translational biomarker discovery in clinical metabolomics: An introductory tutorial. *Metabolomics* **2013,** *9*, 280-299.
64. Xia, J.; Sinelnikov, I.; Wishart, D. S., MetATT - a web-based metabolomic tool for analyzing time-series and two-factor data sets. *Bioinformatics* **2011,** *27*, 2455-2456.
65. Xia, J.; Wishart, D. S., MetPA: a web-based metabolomics tool for pathway analysis and visualization. *Bioinformatics* **2010,** *26*, 2342-2344.
66. Xia, J.; Wishart, D. S., MSEA: a web-based tool to identify biologically meaningful patterns in quantitative metabolomic data. *Nucleic Acids Research* **2010,** *38*, W71-77.
67. Meinhardt, L. W.; Bellato, C. M.; Tsai, S. M., SYBR green I used to evaluate the nuclei number of fungal mycelia. *Biotechniques* **2001,** *31*, 42-46.
68. Graham, D. J.; Castner, D. G., Multivariate analysis of ToF-SIMS data from multicomponent systems: The why, when, and how. *Biointerphases* **2012,** *7*, 49.
69. Smith, H. J.; Schmit, A.; Foster, R.; Littman, S.; Kuypers, M. M.; Foreman, C. M., Biofilms on glacial surfaces: hotspots for biological activity. *npj Biofilms and Microbiomes* **2016,** *2*, 16008.
70. Gamble, L. J.; Anderton, C. R., Secondary ion mass spectrometry imaging of tissues, cells, and microbial systems. *Microscopy Today* **2016,** *24*, 24-31.
71. DeBord, J. D.; Smith, D. F.; Anderton, C. R.; Heeren, R. M. A.; Paša-Tolić, L.; Gomer, R. H.; Fernandez-Lima, F. A., Secondary ion mass spectrometry imaging of Dicytostelium discoideum aggregation streams. *Public Library of Science One* **2014,** *9*, e99319.
72. Sleighter, R. L.; Hatcher, P. G., The application of electrospray ionization coupled to ultrahigh resolution mass spectrometry for the molecular characterization of natural organic matter. *Journal of Mass Spectrometry* **2007,** *42*, 559-574.
73. Jayarathne, T.; Rathnayake, C. M.; Stone, E. A., Local source impacts on primary and secondary aerosols in the Midwestern United States. *Atmospheric Environment* **2016,** *130*, 74-83.
74. Licciardello, A.; Puglisi, O.; Pignataro, S., Effect of organic contaminants on the oxidation kinetics of silicon at room temperature. *Applied Physical Letters* **1986,** *48*, 41-43.
75. Kasi, S. R.; Liehr, M.; Thiry, P. A.; Dallaporta, H.; Offenberg, M., Hydrocarbon reaction with HF-cleaned Si(100) and effects on metal-oxide-semiconductor device quality. *Applied Physical Letters* **1991,** *59*, 108-110.
76. Saga, K.; Hattori, T., Identification and removal of trace organic contamination on silicon wafers stored in plastic boxes. *Journal of the Electrochemical Society* **1996,** *143*, 3279-3284.

77. Budde, K. J.; Holzapfel, W. J.; Beyer, M. M., Application of ion mobility spectrometry to semiconductor technology: Outgassings of advanced polymers under thermal stress. *Journal of the Electrochemical Society* **1995,** *142*, 888-897.
78. Wold, S.; Esbensen, K.; Geladi, P., Principal Component Analysis. *Chemometrics and Intelligent Laboratory Systems* **1987,** *2*, 37-52.
79. Jackson, J. E., Principal components and factor analysis: Part I -- Principal Components. *Journal of Quality Technology* **1981,** *12*, 201-213.
80. Jackson, J. E., *A user's guide to principal components*. John Wiley & Sons, Inc.: New York, NY, 1991.
81. Graham, D. J.; Ratner, B. D., Multivariate analysis of ToF-SIMS spectra from dodecanethiol SAM assembly on gold: Spectral interpretationand ToF-SIMS fragmentation processes. *Langmuir* **2002,** *18*, 5861-5868.
82. Graham, D. J.; Wagner, M. S.; Castner, D. G., Information from complexity: Challenges of ToF-SIMS data interpretation. *Applied Surface Science* **2006,** *252*, 6860-6868.
83. Tyler, B. J.; Rayal, G.; Castner, D. G., Multivariate analysis strategies for processing ToF-SIMS images of biomaterials. *Biomaterials* **2007,** *28*, 2412-2423.
84. Lee, J. L. S.; Gilmore, I. S.; Fletcher, I. W.; Seah, M. P., Multivariate image analysis strategies for ToF-SIMS images with topography. *Surface and Interface Analysis* **2009,** *41*, 653-665.
85. Lee, J. L. S.; Gilmore, I. S.; Seah, M. P., Quantification and methodology issues in multivariate analysis of ToF-SIMS data for mixed organic systems. *Surface and Interface Analysis* **2008,** *40*, 1-14.
86. Mhuireach, G. A.; Betancourt-Román, C. M.; Green, J. L.; Johnson, B. R., Spatiotemporal controls on the urban aerobiome. *Frontiers in Ecology and Evolution* **2019,** *7*, DOI: 10.3389/fevo.2019.00043.
87. Adams, R. I.; Miletto, M.; Taylor, J. W.; Bruns, T. D., Dispersal in microbes: Fungi in indoor air are dominted by outdoor air and show dispersal limitation at short distances. *The ISME Journal* **2013,** *7*, 1262-1273.
88. Bowers, R. M.; McCubbin, I. B.; Hallar, A. G.; Fierer, N., Seasonal variability in airborne bacterial communities at a high-elevation site. *Atmospheric Environment* **2012,** *50*, 41-49.
89. Kokesch-Himmelreich, J.; Schumacher, M.; Rohnke, M.; Gelinsky, M.; Janek, J., ToF-SIMS analysis of osteoblast-like cells and their mineralized extracellular matrix on strontium enriched bone cements. *Biointerphases* **2013,** *8*, 17-29.
90. Invitrogen, Nucleic acids detection and analysis. In *Molecular probes handbook- a guide to fluorescent probes and labeling technologies*, 11 ed.; Invitrogen: Carlsbad, CA, 2018.
91. Rittmann, B. E.; McCarty, P. L., *Environmental biotechnology: principles and applications*. Tata McGraw-Hill Education2012.
92. Madigan, M. T.; Martinko, J. M.; Parker, J., *Brock biology of microorganisms*. Prentice hall Upper Saddle River, NJ1997; Vol. 11.

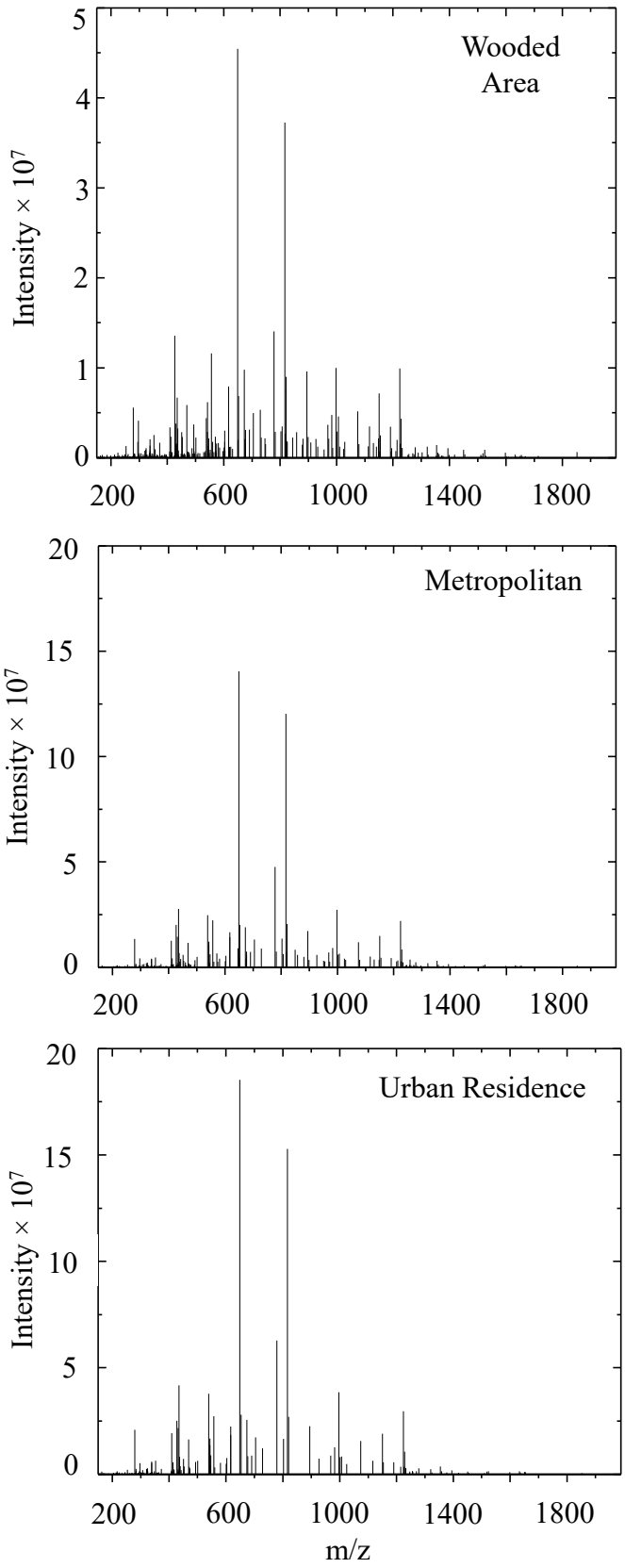

Fig. 1. Representative mass spectra of the wooded area (top), metropolitan (middle), and urban residence (bottom) collection sites deposited for six months. Prevalent peak assignments are presented in Table 1.

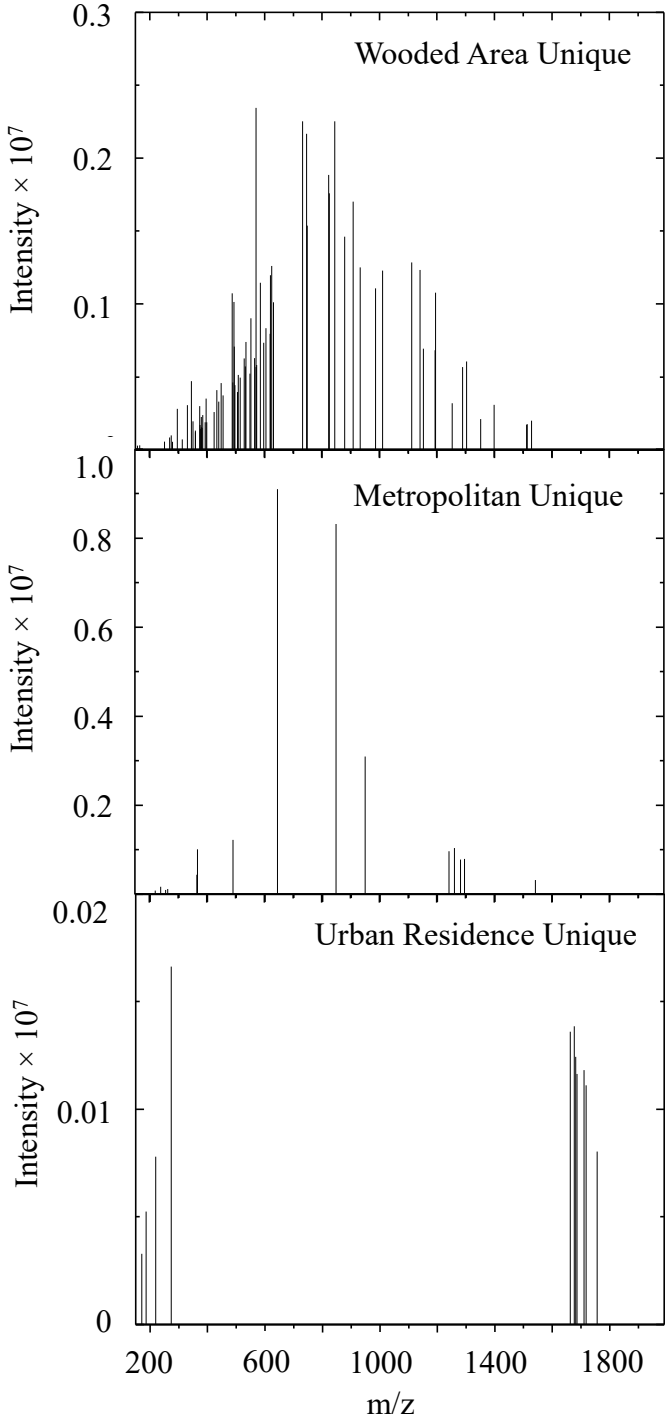

Fig. 2. FTICR-SIMS data showing the unique fragments in the wooded area (top), metropolitan (middle), and urban residence (bottom) collection sites. The deposition time is six months. For each collection site, fragments present at the other two sites are excluded.

	m/z	Molecular Formula (Charge)	Error (ppm)	DBE
Common Peaks	434.7802	$C_{47}H_{81}O_{14}$ (2+)	-1.3	8.5
	538.7291	$C_{47}H_{76}NO_{25}Na$ (2+)	-1.0	10.5
	648.7190	$C_{45}H_{92}O$ (1+)	+7.3	0.5
	778.6532	$C_{42}H_{88}N_3O_9$ (1+)	+2.2	1.0
	816.6004	$C_{45}H_{84}N_3O_6PNa$ (1+)	+1.7	5.5
Wooded Area Unique	570.7996	$C_{48}H_{94}N_4O_{24}P$ (2+)	+0.6	5.5
	732.6312	$C_{42}H_{86}NO_8$ (1+)	-4.9	1.0
	746.6320	$C_{45}H_{85}N_3O_3P$ (1+)	-0.4	6.0
	748.6198	$C_{42}H_{87}NO_7P$ (1+)	-2.2	1.0
	822.5917	$C_{43}H_{84}NO_{13}$ (1+)	-2.5	3.0
	824.5955	$C_{45}H_{85}O_{11}Na$ (1+)	-3.5	3.0
	844.5883	$C_{40}H_{85}N_4O_{12}P$ (1+)	-1.6	1.5
	878.5957	$C_{42}H_{89}NO_{15}P$ (1+)	-0.8	0.0
	908.5749	$C_{47}H_{83}NO_{14}Na$ (1+)	+4.8	6.5
	1112.4678	$C_{47}H_{80}NO_{25}PNa$ (1+)	+2.6	8.5
Metropolitan Unique	364.9061	$C_{51}H_{103}N$ (2+)	+5.8	2.0
	367.8057	$C_{41}H_{82}N_3O_6Na$ (2+)	+3.2	2.5
	490.7996	$C_{44}H_{89}N_2O_{21}$ (2+)	+4.6	2.5
	645.6767	$C_{42}H_{85}N_4$ (1+)	-0.3	3.0
	849.5770	$C_{40}H_{82}N_4O_{13}Na$ (1+)	-0.1	1.5
	950.5510	$C_{43}H_{84}NO_{21}$ (1+)	-2.1	3.0
	1242.3783	$C_{59}H_{68}N_2O_{24}PNa$ (1+)	-0.7	27.0
	1261.3749	$C_{59}H_{66}N_4O_{25}P$ (1+)	+0.1	30.0
	1282.4237	$C_{63}H_{71}N_4O_{23}P$ (1+)	-0.3	31.5
	1296.4678	$C_{60}H_{80}N_3O_{25}PNa$ (1+)	-2.5	22.5
Urban Residence Unique	186.4409	$C_{25}H_{52}O_{11}P$ (3+)	-0.7	2.0
	219.3826	$C_{14}H_{34}N_4O_{25}$ (3+)	-2.7	1.5
	273.3746	$C_{24}H_{36}N_3O_{25}PNa$ (3+)	-2.3	9.5
	1662.2414	$C_{87}H_{176}N_3O_{23}P$ (1+)	-0.8	2.5
	1676.1859	$C_{86}H_{170}N_3O_{25}P$ (1+)	+0.2	4.5
	1682.1635	$C_{87}H_{166}N_4O_{24}P$ (1+)	+0.6	8.0
	1686.1514	$C_{84}H_{167}N_4O_{25}PNa$ (1+)	-2.1	3.5
	1710.1346	$C_{89}H_{163}N_4O_{23}PNa$ (1+)	+0.5	10.5
	1718.1684	$C_{89}H_{169}N_3O_{24}PNa$ (1+)	-2.4	7.0
	1756.1982	$C_{93}H_{173}N_2O_{24}PNa$ (1+)	-1.5	8.5

Table 1. Molecular formula table for the common peaks in the FTICR-SIMS data as well as the peaks unique to each collection site. Formulae are reported along with error and double bond equivalence.

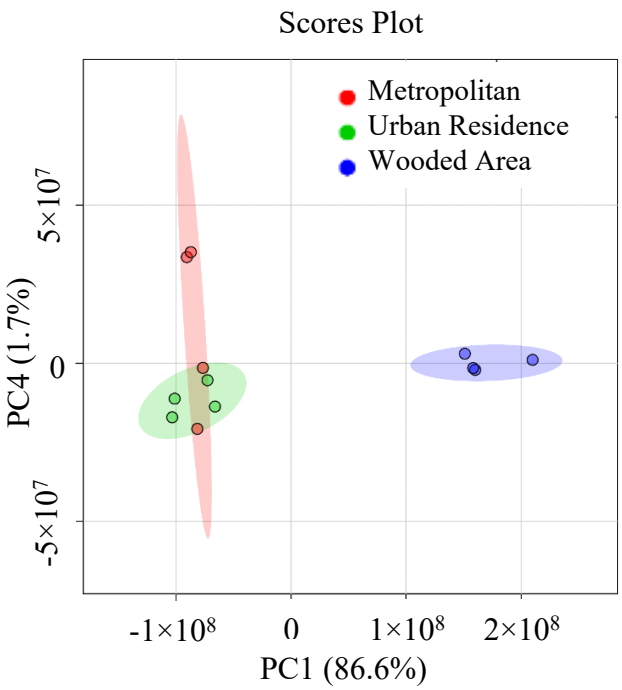

Fig 3. PCA scores plot characterizing the variability between the six-month metropolitan (red), urban residence (green), and wooded area (blue) samples. PC1 shows that spectra from the wooded area site can be separated from the metropolitan and urban residence sites, and PC4 highlights the variability of the metropolitan site. 95% confidence ellipses are also reported for each set of samples. The variance described by the first five PCs is 86.6%, 6.0%, 3.1%, 1.7%, and 1.1%, respectively.

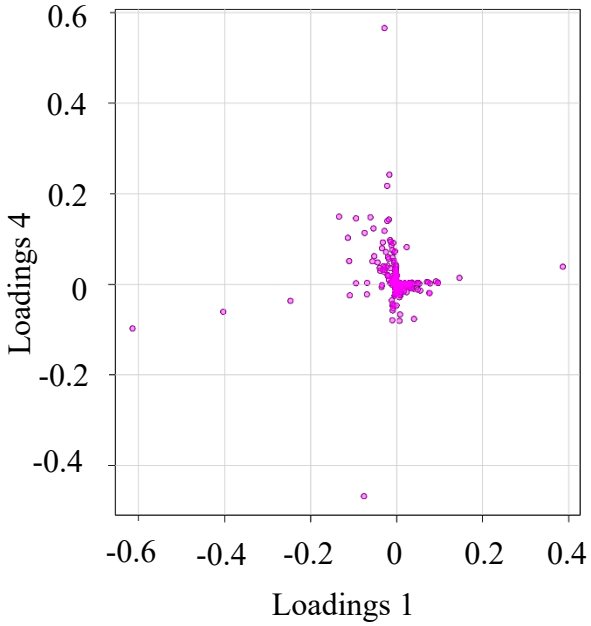

Fig 4. Loading plot of PC1 and PC4 of the six-month samples showing the contribution to the variance for each PC. The loadings indicate that the higher PCs describe variability due to fragments unique to a specific collection site, while the lower PCs describe variable intensity of fragments present on all three samples.

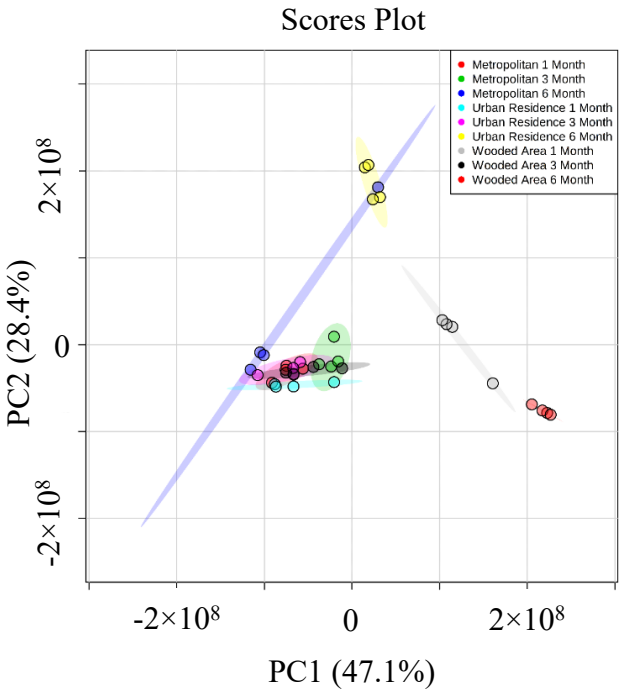

Fig 5. PCA scores plot characterizing the variability between the three collection sites at 1, 3, and 6 months of deposition time. The separation of the 1- and 6-month wooded area site (identified in gray and orange, respectively) and the 6-month urban residence site (yellow) samples suggest seasonal variation may play a role in the chemical profile observed. 95% confidence ellipses are reported for each set of samples. The scores are color coded according to the inset legend. The variance described by the first five PCs is 47.1%, 28.4%, 7.0%, 6.2%, and 2.3%, respectively.

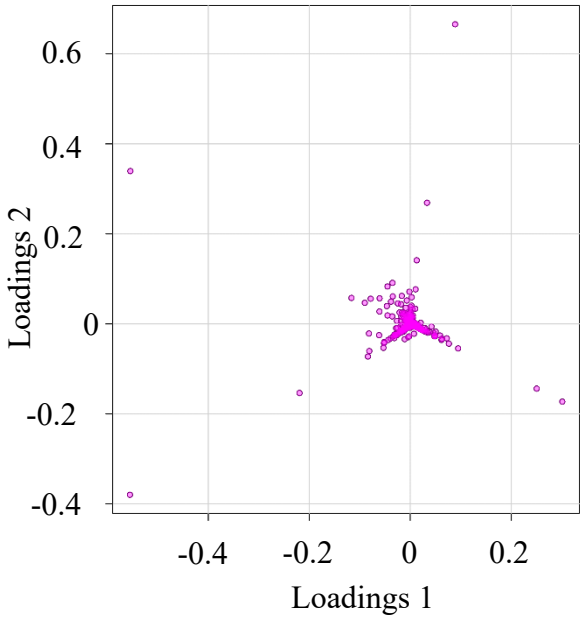

Fig 6. Loading plot of PC1 and PC2 showing the contribution to the variance for each PC. The loadings indicate that the higher PCs describe variability due to fragments unique to a specific collection site, while the lower PCs describe variable intensity of fragments present on all three samples.

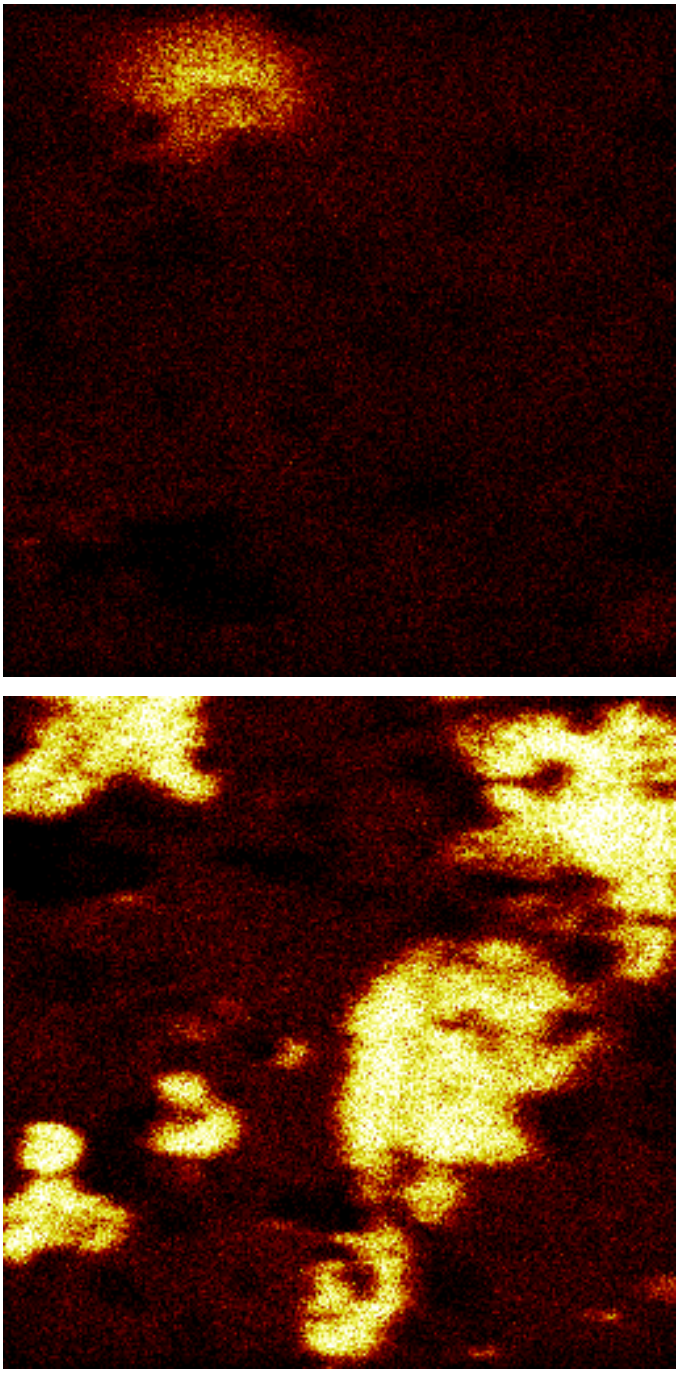

Fig. 7. ToF-SIMS images showing the $C_3H_8N^+$, a secondary ion mass fragment attributed to proteinaceous macromolecules and biomass, collected for three (top) and six (bottom) months at the urban residence site. These images show a build-up of biomass as a function of deposition time and surface coverage. The scale bar is 100 nm for the 500 x 500 nm images, and the ion intensity is scaled to be equivalent for each image.

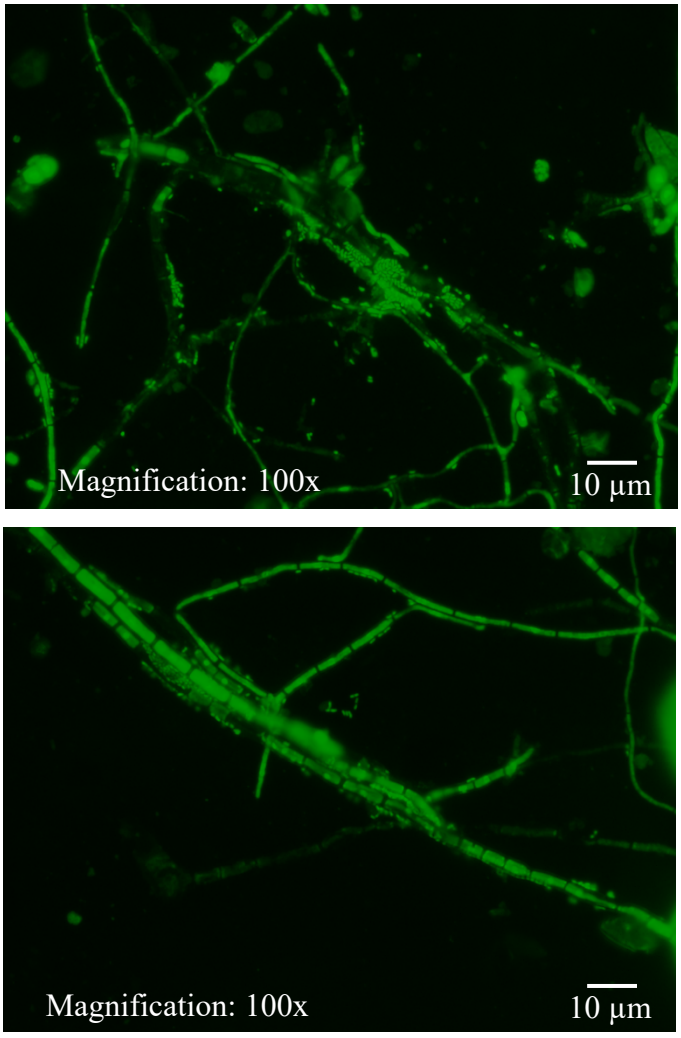

Fig. 8. SYBR-Safe DNA staining images showing the biological presence on the environmental films. Linear cell structures are shown in the top two images, with the nucleus easily visible, that likely correspond to a fungal species. Smaller bacterial species are also observed on the fungal cells.

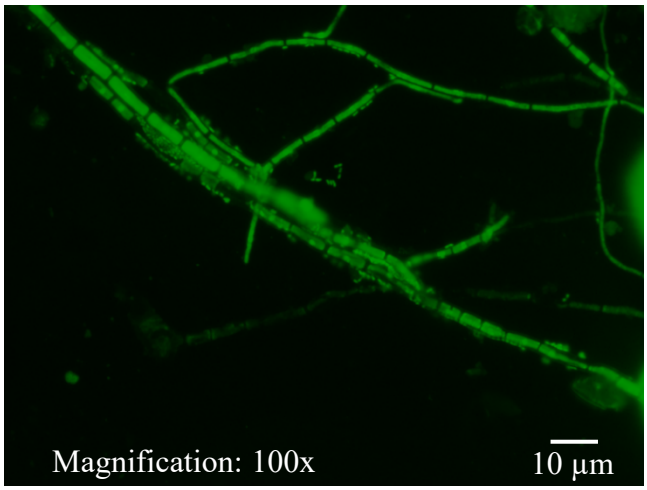

TOC Graphic: For TOC Only